PHYSICAL REVIEW B **80**, 140403(R) (2009)

Anisotropic magnetotransport at the $SrTiO_3/LaAlO_3$ interface

M. Ben Shalom,[1] C. W. Tai,[2,*] Y. Lereah,[2] M. Sachs,[1] E. Levy,[1] D. Rakhmilevitch,[1] A. Palevski,[1] and Y. Dagan[1,†]
[1]*Raymond and Beverly Sackler School of Physics and Astronomy, Tel-Aviv University, Tel Aviv 69978, Israel*
[2]*Department of Physical Electronics, School of Electrical Engineering, The Iby and Aladar Fleischman Faculty of Engineering, Tel-Aviv University, Tel Aviv 69978, Israel*

(Received 7 August 2009; published 8 October 2009)

The sheet resistance as a function of temperature, magnetic field and its orientation for atomically flat $SrTiO_3/LaAlO_3$ interfaces with carrier densities of $\sim 3\times 10^{13}$ cm^{-2} is reported. At low magnetic fields superconductivity is observed below 130 mK. The temperature dependence of the high field magnetoresistance and its strong anisotropy suggest possible magnetic ordering below 35 K. The origin of this ordering and its possible relation to superconductivity are discussed.

DOI: 10.1103/PhysRevB.80.140403 PACS number(s): 75.70.Cn, 73.40.−c

Interface between strongly correlated electron materials can be very different from their constituents. It has been shown that if $LaAlO_3$ (LAO) is epitaxially grown on TiO_2-terminated $SrTiO_3$ (STO) a two-dimensional electron gas (2DEG) is formed at the interface between these insulators.[1] This interface was latter shown to be superconducting[2] and magnetic.[3] Recently Caviglia *et al.* showed that the superconducting transition temperature can be controlled by solely varying the number of charge carriers at the interface using a gate voltage.[4] These unexpected results and the potential for high performance oxide based electronics motivated an effort to understand the properties of this interface[5–7] and to improve it.

The origin of the large carrier concentration at the interface remains under debate. When depositing monolayers of LAO on STO conductivity appears only for a TiO_2 terminated surface[1] at a threshold of four unit cells.[8] These observations suggest that the electrostatic structure of the interface: nonpolar STO planes covered with alternatingly charged planes on the LAO side should lead to an interfacial reconstruction. This reconstruction can be dominantly electronic in nature,[9,10] or partly due to cationic mixing.[5] A lattice distortion driven by the polar nature of the interface has also been proposed.[11] Other papers suggested that oxygen vacancies play a major role in creating high carrier densities.[6,12,13] It seems that the latter effect is insignificant for samples deposited at pressure range of $10^{-5}-10^{-3}$ Torr.[2,14,15]

Magnetic effects have been theoretically predicted for STO/LAO interfaces.[7,16] Recent observations of magnetic hysteresis below 0.3 K along with MR oscillations with periodicity proportional to $\sqrt{B}$ have been explained in terms of commensurability of states formed at the terrace edges of the STO.[17]

While superconductivity in this interface has been shown to be 2D in nature[2] the way such interface can exhibit magnetic properties is still a puzzle. In this Rapid Communication we show that for carrier concentrations of 3×10^{13} cm^{-2} the 2DEG is superconducting at 130 mK, yet, anusual magnetotransport effects are observed below 35 K. Our data support possible evidence for a magnetic order formed below this temperature. A magnetic impurities scenario is ruled out.

Eight unit cells of LAO were deposited from a single-crystal target onto a TiO_2-terminated STO substrates (tolerance $<0.3°$) prepared in a similar way as described by Koster *et al.*[18] by pulsed laser deposition. We use pulse rate of 1Hz and energy density of 1.5 $J\,cm^{-2}$ at oxygen pressure ranging between $1\times 10^{-3}-5\times 10^{-5}$ Torr and temperature of 800 °C. The deposition was monitored by reflection high energy electron diffraction (RHEED). The maxima of the RHEED intensity oscillations indicate a complete layer formation and used as a measurement for the sample thickness [Fig. 1(b)]. One of the samples was imaged by a high-resolution transmission electron microscope revealing a high quality interface and confirming the thickness measurement by the RHEED [Fig. 1(a)]. The 2DEG underneath the LAO

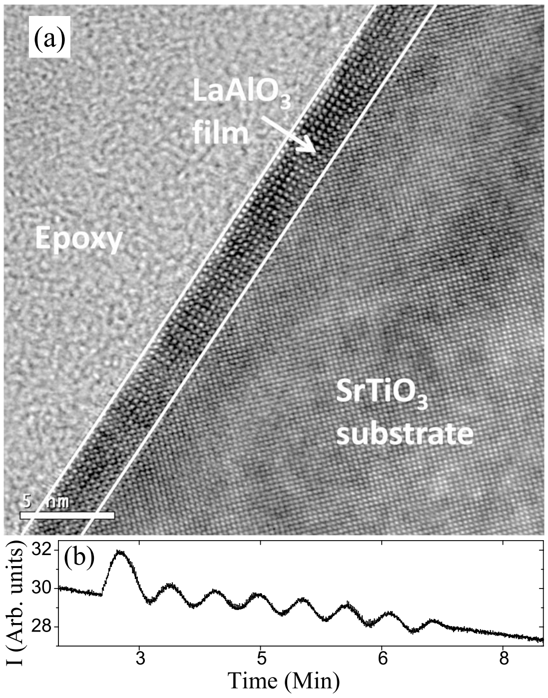

FIG. 1. (a) High resolution transmission electron microscopy image of STO/LAO interface. The lines outline the LAO film boundaries. The number of layers is as expected from the number of RHEED oscillations. (b) RHEED intensity oscillations indicating deposition of eight unit cells.

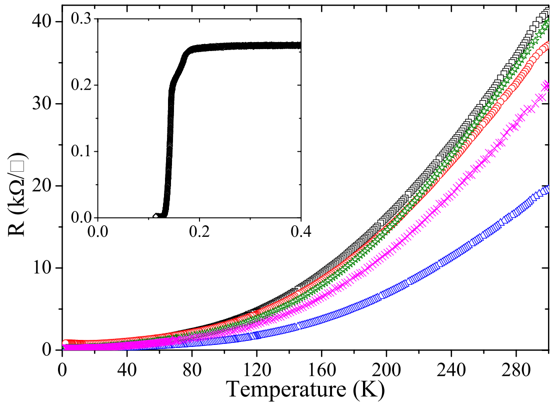

FIG. 2. (Color online) The sheet resistance as a function of temperature for three typical samples: sample1 (black squares), sample 2 (red circles), sample 3 (blue triangles), and the two bridges of sample 4 (green stars, magenta crosses). Insert: sheet resistance vs temperature for sample 1.

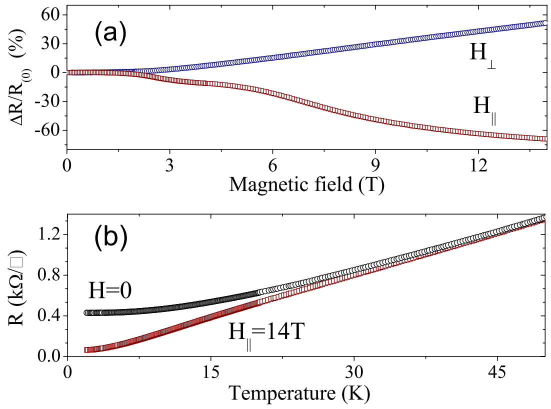

FIG. 3. (Color online) Sample 1 (a) blue circles: the MR as a function of magnetic field applied perpendicular to the interface. Red squares are the MR data for field applied along the interface parallel to the current. (b) The sheet resistance as a function of temperature at zero field (black circles) and at 14 T applied parallel to the current (red squares)

layers was electrically connected using a wire bonder. One of the samples was patterned using reactive ion etch (RIE) into Hall bars with bridges dimensions of 50×750 microns squared. The bridges were align perpendicular or parallel to the terrace edges. Other samples were connected in a Van-Der-Pauw (VDP) geometry for resistivity and Hall measurements, or in a strip geometry (with dimensions of about 2×0.1 mm) when the current direction had to be well defined.

In this Rapid Communication we present four typical samples deposited at oxygen pressures of 5×10^{-5} (sample 1), 1×10^{-4} (samples 2 and 4), and 9×10^{-4} (sample 3), with carrier concentrations of 3, 5, 2, and 3.5×10^{13} cm^{-2} for samples 1–4, respectively, as inferred from Hall measurements at 2 K. The charge carrier density has a very weak temperature dependence of up to 100 K. This is in contrast with the strong temperature dependence reported in Ref. 3.

The sheet resistance as a function of temperature for these samples is shown in Fig. 2. All samples under study including all bridges in the patterned sample exhibit similar transport properties. The fact that small bridges and VDP measurements resulted in similar features is indicative of the samples' homogeneity. We also note that the variation of oxygen pressure during deposition resulted in a rather small change in carrier concentration and resistivity. Sample 1 was also measured in a dilution refrigerator and was shown to be superconducting with the transition temperature $T_c=130$ mK (insert of Fig. 2).

The magnetoresistance (MR) is defined as $\frac{\Delta R}{R_0}=\frac{R(\mathbf{H})-R(H=0)}{R(H=0)}$, where $R(\mathbf{H})$ is the resistance at a magnetic field $\mathbf{H}$. It is presented for $T=2$ K in Fig. 3(a). When $\mathbf{H}$ is applied perpendicular to the film a positive MR is observed (blue circles). The data are an average between positive and negative fields in order to eliminate spurious Hall contribution. By contrast a large negative MR is seen for fields parallel to the film and to the current (red squares). We note that both the positive and negative MR are very large, 50% and 70%, respectively, for $H=14$ T. We also note that for perpendicular fields no hysteresis is observed down to 130 mK where superconductivity shows up.

In Fig. 3(b) we show the temperature dependence of the (parallel) negative MR. The black circles are the zero-field measurement and the red circles are data taken at 14 T applied parallel to the current $\mathbf{J}$. We emphasize that the negative MR disappears above 35 K. The large negative MR and its strong anisotropy suggest strong magnetic scattering in the plane. To further investigate this assumption we rotated $\mathbf{H}$ around a horizontal axis changing its angle with the normal to the interface while keeping the field's amplitude constant (14 T).

In Fig. 4 the MR at 14 T is plotted as a function of φ (see illustration). $\varphi=90°$ corresponds to $\mathbf{H}\parallel\mathbf{J}$. The dip is extremely sharp and the MR changes sign at 87° (93°).

We shall now check for anisotropy in the plane of the interface. In Fig. 5 the resistance as a function of angle between the magnetic field and the current is shown for various temperatures. $\theta=90°$ corresponds to $\mathbf{H}\perp\mathbf{J}$ applied parallel to the film [Fig. 5(b)]. At 40 K the resistance is maximum for $\mathbf{H}\perp\mathbf{J}$. The dashed black line Fig. 5(a) is a fit using

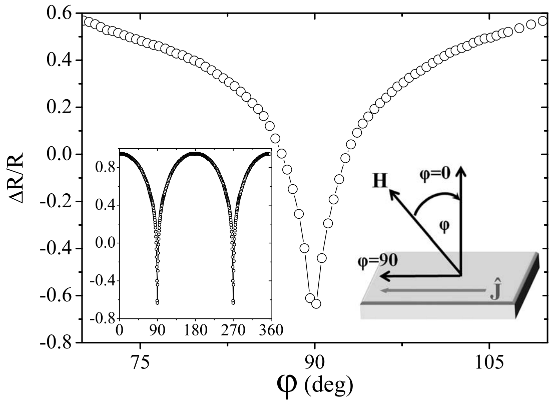

FIG. 4. Sample 2, the MR as a function of the angle φ between the perpendicular to the interface and the magnetic field (φ is depicted at the right insert). Left Insert: full angle scan.

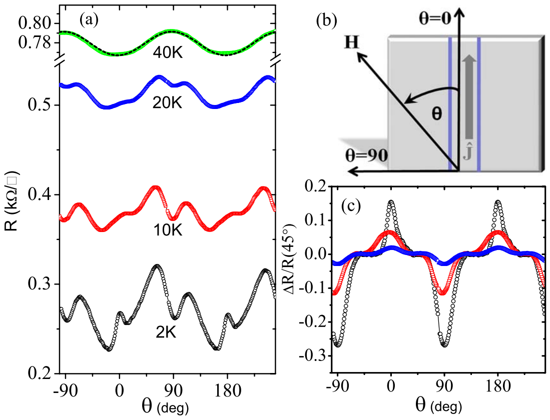

FIG. 5. (Color online) Sample 3 (a) The sheet resistance at 14 T as a function of angle between **H** and **J** at various temperatures. The dashed line is a $\sin^2(\theta)$ fit (see text for details) (b) Illustration of the measurement geometry. (c) The same data as in (a) after subtracting the fit and normalizing with the measured resistance at $\theta=45°$. This procedure uncovers the (in-plane) anisotropic MR.

$R(\theta,T)=r(T)\sin^2(\theta)+R_0(T)$, with θ being the angle between **H** and the **J**, $r(T=40\ \mathrm{K})=25\ \Omega$ and $R_0(T=40\ \mathrm{K})=767\ \Omega$. This simple dependence persists up to above 100 K. As elaborated in the discussion below we attribute this behavior to geometric effects related to the 2D nature of the electron gas at the interface.

Below 40 K another effect appears. Focusing for example on the 20 K data, a dip appears at ±90° while a peak is revealed at 0 and 180°. At 10 K and below the latter effect becomes even larger than the $\sin^2(\theta)$ and significant maxima (minima) appear at 0 and 180° (90 and −90°). We note that since the interface is probably not perfectly parallel to the field a small Hall contribution results in a small deviation between zero and 180° Moreover such a small deviation can result in a perpendicular component, although this component is minute its influence can be non-negligible and should add up to the $\sin^2(\theta)$ effect. To eliminate the Hall contribution we symmetrized the data for positive and negative fields. To remove the contributions with the $\sin^2(\theta)$ dependencies we subtracted the fit $R(\theta,T)=r(T)\sin^2(\theta)+R_0(T)$ from the 2, 10, and 20 K data $r(T)$ and $R_0(T)$ were determined for each temperature. This procedure uncovers the (in-plane) anisotropic MR. The resulting data normalized with the measured resistance at $\theta=45°$ are shown in Fig. 5(c). We note a sharp peak when $\mathbf{H}\parallel\mathbf{J}$ and a sharp dip appears for $\mathbf{H}\perp\mathbf{J}$. A similar effect is seen for a different strip rotated by 90° (not shown). As elaborated below we interpret this effect as being the anisotropic MR. A small-angle deviations between temperatures could be due to the rotator backlash.

We shall now discuss the MR data from Figs. 3–5. We first note that the amplitudes of both negative and positive MR in Fig. 3(a) are very large. The positive MR for **H** perpendicular to the interface could be due to orbital effects that have a significant contribution since $\omega_c\tau$ is close to unity, where ω_c is the cyclotron frequency and τ the scattering time. For $\mathbf{H}\parallel\mathbf{J}$ such orbital effects are not existent. Yet, the MR is even larger, 70%. The relevant mechanisms that can produce negative MR are: 2D weak localization, magnetic impurities and the magnetic nature of the material itself. The first effect is ruled out since it is usually small (of the order of a few percents) and appears for **H** applied perpendicular to the film. The second effect is usually isotropic, in strong contrast with our results. We are therefore led to conclude that the large negative MR we observe is due to a magnetic order formed at the interface.

We emphasize that the negative MR seen in Fig. 3(a) for $\varphi=90°$ is very different from the negative isotropic MR reported in Ref. 3. The MR versus φ dependance shown in Fig. 4 is extremely sharp around $\varphi=90°$. This is a key observation in our Rapid Communication. The fact that the MR changes sign for a variation of 3° implies that a small perpendicular field component is sufficient to mute the mechanism responsible for the parallel negative MR. This is due to the fact that when $\varphi=93°$ the parallel field component is almost unchanged (13.98 T) while the perpendicular component is only 0.73 T. Such a component is too small to induce any orbital effect as can be seen in Fig. 3(a). One may claim that the positive orbital MR for 0.73 T is in fact larger, yet overwhelmed by a large isotropic negative MR. However, when measuring the negative MR with $\mathbf{H}\parallel\mathbf{J}=0.73\ \mathrm{T}$ we find it to be very small [Fig. 3(a)]. Hence this scenario is ruled out. We therefore conclude that there is a strong strange anisotropy of the MR. The only element in our system with such strong directionality is the interface itself. We therefore conclude that the strong φ dependence gives possible evidence for the existence of magnetic order confined to a few layers near the interface. This magnetic order in the interface vanishes above 35K according to the data in Fig. 3(b) for the carrier density and LAO thickness under study.

Further evidence for the quasi-2D nature of the conducting interface can be found from the in-plane angular dependence of the MR as presented in Fig. 5 at 40 K. For this geometry (field and current in plane) the Lorentz force is perpendicular to the interface. Assuming a quasi-2D confinement one expects an enhancement of scattering for $\mathbf{H}\perp\mathbf{J}$ assuming that the band structure is not very simple. This *positive* orbital contribution to the MR should be quadratic in the field component that is perpendicular to **J**. We observed a $\sin^2(\theta)$ behavior as expected (dashed line Fig. 5).

We can roughly estimate the width of the confinement zone using a naive calculation with the mean-free path at low temperatures $\ell=\frac{h}{e^2k_FR_\square}\approx 25\ \mathrm{nm}$ at 2 K, the Fermi wave number $k_F=\sqrt{2\pi n_s}$, e the electron charge, $R_\square$ the sheet resistance, and n_s the carrier density. The ratio between this MR and the one observed when **H** is applied perpendicular to the interface should be proportional to $(d/\ell)^2$ where d is the size of the confinement zone. Substituting the values for $R_\square$ and the amplitude of the two orbital effects at 40 K we obtain $d\approx 1-2\ \mathrm{nm}$. This gives the right order of magnitude for the width of the confinement zone. We note that this effect and all other effects reported here are similar for current running parallel or perpendicular to the substrate terraces, which rules out the terraces as their origin in contrast with ref.[17]

In summary, the temperature field and orientation dependence of the MR of sharp STO/LAO interfaces is reported. Four contributions to the MR are identified: (a) an orbital one, measured when **H** is perpendicular to the interface, (b) the $\sin^2(\theta)$ MR persisting up to rather high temperatures. This MR appears when **H** is applied parallel to the interface and $\mathbf{H}\perp\mathbf{J}$. We relate it to the finite size of the confinement zone. This MR is also positive, but its amplitude comparing to the previous effect is smaller by a factor proportional to $(d/\ell)^2$. (c) The more interesting MR appears below 35 K. This, negative, low-temperature MR appears when **H** is applied exactly parallel to **J**. It cannot be due to orbital effects and its large (negative) magnitude suggests that it has a magnetic origin. (d) the last effect is seen when rotating the field in plane. Below 35 K anisotropic MR appears. It has a maximum for $\theta=0$ ($\mathbf{H}\parallel\mathbf{J}$). Its amplitude increases as the temperature decreases. We interpret this MR as being the anisotropic MR expected for magnetic materials.[19] Scattering resulting from spin-orbit interactions becomes stronger when the electron travels parallel to the magnetization as seen in Fig. 5(c). The latter two effects: the strong (parallel) negative MR and the anisotropic, in-plane MR show up *together* below 35 K. Below this temperature a magnetic phase emerges. This phase is extremely sensitive to an out-of-plane magnetic field. This sensitivity is unclear to us, yet, it rules out magnetic impurities as the origin of the effects and suggests that the magnetic order is confined to the vicinity of the interface. We take note of the following observations: both the parallel negative MR and the anisotropic, in-plane MR exhibit no saturation up to 14 T, and we were not able to observe magnetic hysteresis down to $T_c=130$ mK. In view of these observations and due to the occurrence of superconductivity at low temperatures it is difficult to believe that the interface is ferromagnetic. The nature of the magnetic order formed and whether it coexist with superconductivity still need further investigations. One possibility is that the magnetic order observed is induced by the magnetic field itself below 35 K. This temperature may vary with number of charge carriers and film thickness. A second option is that antiferromagnetic order is formed at the interface with a $T_N=35$ K. If the latter is correct then this system may be another example for coexistence of superconductivity and antiferromagnetism such as heavy fermion materials.[20]

We thank A. Aharony, G. Deutscher, A. Gerber, S. Hacohen-Gourgy, O. Entin-Wohlman, and Y. Yacoby for useful discussions. This research was partially supported by the Israel Science Foundation (ISF) by the FIRST program of the ISF and by the Wolfson family charitable trust. C.W.T. is grateful for the financial support by European Commission (Grant No. 29637).

---

[*] Present address: Arrhenius Laboratory, Stockholm University, Sweden.

[†] yodagan@post.tau.ac.il

[1] A. Ohtomo and H. Y. Hwang, Nature (London) **427**, 423 (2004).

[2] N. Reyren *et al.*, Science **317**, 1196 (2007).

[3] A. Brinkman, M. Huijben, M. van Zalk, J. Huijben, U. Zeitler, J. C. Maan, W. G. van der Wiel, G. Rijnders, D. H. A. Blank, and H. Hilgenkamp, Nature Mater. **6**, 493 (2007).

[4] A. D. Caviglia, S. Gariglio, N. Reyren, D. Jaccard, T. Schneider, M. Gabay, S. Thiel, G. Hammerl, J. Mannhart, and J.-M. Triscone, Nature (London) **456**, 624 (2008).

[5] P. R. Willmott *et al.*, Phys. Rev. Lett. **99**, 155502 (2007).

[6] G. Herranz *et al.*, Phys. Rev. Lett. **98**, 216803 (2007).

[7] Z. Zhong and P. J. Kelly, EPL **84**, 27001 (2008).

[8] S. Thiel, G. Hammerl, A. Schmehl, C. W. Schneider, and J. Mannhart, Science **313**, 1942 (2006).

[9] S. Okamoto and A. J. Millis, Nature (London) **428**, 630 (2004).

[10] Z. S. Popović, S. Satpathy, and R. M. Martin, Phys. Rev. Lett. **101**, 256801 (2008).

[11] R. Pentcheva and W. E. Pickett, Phys. Rev. Lett. **102**, 107602 (2009).

[12] A. Kalabukhov, R. Gunnarsson, J. Börjesson, E. Olsson, T. Claeson, and D. Winkler, Phys. Rev. B **75**, 121404(R) (2007).

[13] W. Siemons, G. Koster, H. Yamamoto, W. A. Harrison, G. Lucovsky, T. H. Geballe, D. H. A. Blank, and M. R. Beasley, Phys. Rev. Lett. **98**, 196802 (2007).

[14] N. Nakagawa, H. Y. Hwang, and D. A. Muller, Nature Mater. **5**, 204 (2006).

[15] M. Huijben, G. Rijnders, D. H. A. Blank, S. Bals, S. Van Aert, J. Verbeeck, G. Van Tendeloo, A. Brinkman, and H. Hilgenkamp, Nature Mater. **5**, 556 (2006).

[16] R. Pentcheva and W. E. Pickett, Phys. Rev. B **74**, 035112 (2006).

[17] M. van Zalk, J. Huijben, A. Giesbers, M. Huijben, U. Zeitler, J. Maan, W. Vanderwiel, G. Rijnders, D. Blank, H. Hilgenkamp, and A. Brinkman, arXiv:0806.4450 (unpublished).

[18] G. Koster, B. L. Kropman, G. J. H. M. Rijnders, D. H. A. Blank, and H. Rogalla, Appl. Phys. Lett. **73**, 2920 (1998).

[19] T. R. McGuire and R. I. Potter, IEEE Trans. Magn. **11**, 1018 (1975).

[20] N. D. Mathur, F. M. Grosche, S. R. Julian, I. R. Walker, D. M. Freye, R. K. W. Haselwimmer, and G. G. Lonzarich, Nature (London) **394**, 39 (1998).